

Effectiveness of parton cascade in solving the relativistic Boltzmann equation in a box

Todd Mendenhall^{1,2} and Zi-Wei Lin^{1,*}

¹*Department of Physics, East Carolina University, Greenville, NC 27858, USA*

²*Applied Research Associates, Inc., Raleigh, NC 27615, USA*

(Dated: August 1, 2025)

We benchmark the ZPC parton cascade with an exact analytical solution of the relativistic Boltzmann equation for a homogeneous and massless gas with a constant and isotropic elastic cross section. We measure the accuracy of ZPC with the relative mean deviation between its momentum distribution and the exact solution. We use two generalized collision schemes to further improve the accuracy of ZPC over the recent t -minimum collision scheme. We find that ZPC can reproduce very well the time evolution of the single-particle distribution function for the exact solution's initial condition, with one generalized collision scheme giving an accuracy better than 1% for the momentum distribution at any time in all studied cases, including very high opacities where naively the parton cascade approach is expected to fail.

INTRODUCTION

A new phase of matter with parton degrees of freedom called the quark-gluon plasma (QGP) has been formed in high-energy nuclear collisions at the Relativistic Heavy Ion Collider [1] and the Large Hadron Collider [2]. The STAR Collaboration has shown that the matter formed in Au+Au collisions at $\sqrt{s_{NN}} = 3$ GeV collisions is dominated by hadronic interactions [3], while by $\sqrt{s_{NN}} = 4.5$ GeV there is evidence [4] for the onset of dominant partonic interactions from the observation of the constituent quark number scaling [5]. There has also been evidence that the QGP is even formed in small collision systems such as d+Au collisions at RHIC [6–8] as well as p+p and p+Pb collisions at the LHC [9, 10]. It is thus important to study small systems or systems at lower energies to establish the origin of collectivity and to reliably extract the QGP properties. The hydrodynamics approach has been very successful in describing large systems at high energies; however, it is not clear whether it can be applied to small or low energy systems [11–13]. For a small system, we expect the non-equilibrium dynamics to be important, such as the parton escape mechanism [14–16] for the generation of anisotropic flows. Transport models [17–19] and effective kinetic theory [20] are natural tools to address non-equilibrium dynamics.

Therefore, it is important to be able to accurately model the parton dynamics of the QGP. At very high temperatures, quarks and gluons are weakly interacting due to asymptotic freedom, where the QGP could be pictured as a relativistic gas as described by the relativistic Boltzmann equation (RBE). The RBE gives the evolution of the single-particle distribution function $f(x^\mu, p^\mu, t)$ and has a wide range of applications from heavy ion collisions [17–22] to core-collapse supernovae [23]. Because the RBE is a complicated non-linear integro-differential equation, exact analytical solutions of the RBE are rare. Numerical or approximate solutions of the RBE are more common, such as solutions under the relaxation time approximation [24].

Zhang's parton cascade (ZPC) [17] is a Monte Carlo program that uses the cascade method to numerically solve the RBE under two-to-two parton scatterings. In general, parton cascades suffer from causality violation at high densities [25–27], which arises due to the geometric interpretation of the cross section σ . Thus, one naively expects ZPC to be accurate only in the dilute limit when the interaction length $\sqrt{\sigma/\pi}$ is much smaller than the mean free path l , i.e., when $\chi \ll 1$ with $\chi = \sqrt{\sigma/\pi}/l$ being the opacity [28]. The parton subdivision method can be used to reduce the inaccuracies that originate from the causality violation [29]. Parton subdivision can be understood in terms of the transformation $f \rightarrow f \times l_{\text{sub}}$ and $d\sigma/dt \rightarrow d\sigma/dt/l_{\text{sub}}$ [30], under which the RBE is invariant. With the subdivision factor $l_{\text{sub}} > 1$, this transformation decreases the opacity by $\chi \rightarrow \chi/\sqrt{l_{\text{sub}}}$ [28, 30] and can thus reduce the causality violation. However, this parton subdivision method is computationally expensive, because the parton number per event increases as $N \rightarrow N \times l_{\text{sub}}$ and the number of collisions to simulate each event increases by a factor of l_{sub}^2 . Recently we found a new parton subdivision transformation [30] for particles in a box with periodic boundary conditions, where we increase f by decreasing the volume as $V \rightarrow V/l_{\text{sub}}$. This new transformation is much faster since the parton number per event remains the same [30], but it can only be applied to box simulations. Because the parton subdivision method changes the event-by-event fluctuations and correlations [30], which are important observables for the study of nuclear collisions, we need a parton cascade that accurately solves the RBE without using the parton subdivision method.

In ZPC or any parton cascade, there are different scattering prescriptions to implement the cascade method that generally lead to different results [17, 26]. A scattering prescription, or collision scheme, refers to the choice of the collision frame, the collision space-time point(s), the ordering frame, and the ordering time [17]. Whether a collision happens is determined in the collision frame with the closest approach criterion, while possible colli-

sions are ordered according to the ordering time (in the ordering frame) and performed in that order. The ZPC uses the two-parton center-of-momentum frame as the collision frame, while the ordering frame is taken as the rest frame of the gas (i.e., the global frame) [17]. Although the collision time is a single value in the collision frame, the two partons generally have different spatial coordinates at that time due to the finite σ , which then lead to two different times of collision $t_{c,1}$ and $t_{c,2}$ in the global frame after Lorentz transformations [30]. With the collision frame and ordering frame fixed, there are still different choices for the collision time and ordering time, leading to different collision schemes. Note that each of the two partons involved in a collision changes its momentum at the chosen collision time at its corresponding position in the global frame.

Recently, it was shown that the inaccuracy from the causality violation depends greatly on the collision scheme [30]. In the original ZPC [17], the ordering time and collision times for both partons are all chosen as $(t_{c,1} + t_{c,2})/2$, thus this original collision scheme is called the t -average scheme. Various collision schemes have been studied with ZPC, and a new collision scheme was found to perform much better than the original scheme [30]. The new scheme chooses the ordering time and the parton collision times as $\min(t_{c,1}, t_{c,2})$, so it is called the t -minimum scheme. This new collision scheme significantly improves the accuracy, as judged from comparisons with the expected thermal distribution in equilibrium as well as the time evolution of the momentum distribution in comparison with the parton subdivision results [30]. Since the latter depends on the assumption that the subdivision results are correct, it is better to compare ZPC with an exact analytical solution of the RBE. While an analytical solution of the non-relativistic Boltzmann equation for a homogeneous gas has long been known [31], an exact analytical solution for a relativistic massless gas was found only recently [32, 33]. Then the hadron transport SMASH was compared with this exact solution, where good agreement was observed [34]. In this study, we assess and then improve the accuracy of ZPC by comparing with this exact solution for the time evolution of the full momentum distribution of a massless homogeneous gas.

EXACT ANALYTICAL SOLUTION OF THE RBE

The recent exact analytical solution of the RBE [32, 33] for a massless, homogeneous and isotropically expanding gas, which scatters with an energy-independent and

isotropic elastic cross section, is given by

$$f(p, \tau) = \lambda \exp \left[-\frac{u^\mu p_\mu}{T(\tau) \kappa(\tau)} \right] \times \left[\frac{4\kappa(\tau) - 3}{\kappa^4(\tau)} + \frac{u^\mu p_\mu}{T(\tau)} \frac{1 - \kappa(\tau)}{\kappa^5(\tau)} \right]. \quad (1)$$

Here, p^μ is the four-momentum, λ is the fugacity, u^μ is the four-velocity of the gas, and $\kappa(\tau) = 1 - \exp(-\tau/6)/4$. The temperature $T(t) = T(0)/a(t)$ depends on a time-dependent scale factor $a(t)$, which controls the spatial expansion in the Friedman-Lemaître-Robertson-Walker (FLRW) metric $ds^2 = dt^2 - a^2(t)(dx^2 + dy^2 + dz^2)$. The time variable is $\tau = \int_{\hat{t}_0}^{\hat{t}} dt'/a^3(t')$, where the scaled time is $\hat{t} = t/l$ [32] with l being the mean free path.

The single-particle distribution function is independent of the spatial coordinates and is spherically symmetric in the momentum space: $f(x^\mu, p^\mu, \tau) \rightarrow f(p, \tau)$, where p represents the magnitude of momentum. The exact solution of Eq. (1) has the following initial condition corresponding to $\tau = 0$ when $T(0) = T_0$:

$$f(p, 0) = \lambda \frac{256}{243} \frac{p}{T_0} \exp \left(-\frac{4p}{3T_0} \right). \quad (2)$$

RESULTS

The exact analytical solution is also valid for a constant scale factor $a(t) = 1$. So in this study we investigate this non-expanding case, which corresponds to box calculations with periodic boundary conditions [17]. Note that in this case the temperature of the system remains constant at $T(\tau) = T$, and we choose $\lambda = 1$ for the fugacity. Then the time evolution of Eq. (1) can be simplified as

$$f(p, \tau) = \exp \left[-\frac{p}{T \kappa(\tau)} \right] \left[\frac{4\kappa(\tau) - 3}{\kappa^4(\tau)} + \frac{p}{T} \frac{1 - \kappa(\tau)}{\kappa^5(\tau)} \right]. \quad (3)$$

It approaches the thermal distribution at late times:

$$f_{\text{eq}}(p) \equiv f(p, \tau \rightarrow \infty) = \lambda \exp \left(-\frac{p}{T} \right). \quad (4)$$

The evolution of a parton system depends on the density and cross section and thus the system approaches equilibrium at different rates [30]. The scaled time \hat{t} [32] takes this into account, where $\tau = \hat{t}$ for our choice of $a(t) = 1$ and $\hat{t}_0 = 0$. For gluons under the Boltzmann statistics, the momentum distribution is higher by the gluon degeneracy factor, and the opacity is given by [28]

$$\chi = \frac{16}{\pi^2} T^3 \sqrt{\frac{\sigma^3}{\pi}}. \quad (5)$$

As a result, the time variable τ is related to the global time t and opacity χ as

$$\tau = t T \left(\frac{16\chi^2}{\pi} \right)^{\frac{1}{3}}. \quad (6)$$

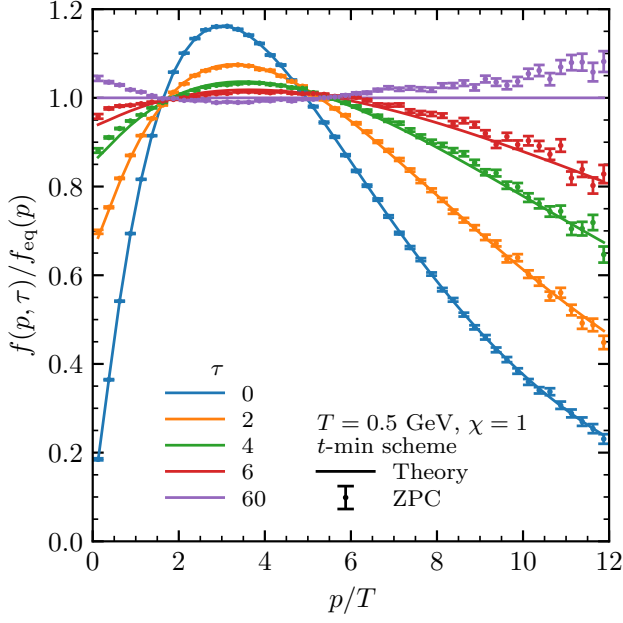


FIG. 1. Ratio of $f_{\text{ZPC}}(p, \tau)$ and $f_{\text{Theory}}(p, \tau)$ over the equilibrium distribution $f_{\text{eq}}(p)$ versus p/T at various times for gluons in a box at $T = 0.5$ GeV and $\sigma = 1.65$ mb (for $\chi = 1.0$), where $f_{\text{ZPC}}(p, \tau)$ comes from ZPC with the t -minimum collision scheme and $f_{\text{Theory}}(p, \tau)$ represents the exact solution.

In this study, we run ZPC until an ending time of $\tau = 60$ because this time is long enough for each system to practically reach equilibrium. For each configuration, we start ZPC at $\tau = 0$ from the initial condition of Eq. (2), and we use 1000 events with 16000 gluons per event to ensure that the results are statistically reliable.

In Fig. 1, we examine the ZPC results from the t -minimum scheme by plotting the ratio $f(p, \tau)/f_{\text{eq}}(p)$ as a function of p/T at several τ during the evolution for a gluon gas at $T = 0.5$ GeV and $\sigma = 1.65$ mb. The symbols represent the ratio of the ZPC distributions $f_{\text{ZPC}}(p, \tau)$ over the equilibrium distribution of Eq. (4), while the solid lines represent the ratio of the analytical distributions $f_{\text{Theory}}(p, \tau)$ over the equilibrium distribution. Note that the ZPC distributions are obtained at discrete values of p/T , while the analytical (including the equilibrium) distributions are smooth functions of p/T . For apple-to-apple comparisons, for both $f_{\text{Theory}}(p, \tau)$ and $f_{\text{eq}}(p)$ we calculate the bin-averaged value as $f(p_i) \equiv \int_a^b f(p) d^3p / \int_a^b d^3p$, where $a = p_i - \Delta p/2$ and $b = p_i + \Delta p/2$ with a constant bin width Δp .

We see in Fig. 1 that the initial distribution at $\tau = 0$ is higher than the equilibrium distribution for $p/T \in [1.64, 4.96]$ while lower in other p/T ranges. Since we have implemented the initial condition of Eq. (2) in ZPC, $f_{\text{ZPC}}(p, 0)$ fully agrees with $f_{\text{Theory}}(p, 0)$ as intended. As τ increases, particle collisions cause the system to approach equilibrium, and the exact solution is seen to

reach equilibrium by $\tau = 60$. We see that the time evolution of the ZPC momentum distributions at early time agrees very well with the exact solution. At late times, however, the ZPC momentum distribution under the t -minimum scheme shows a underpopulation within $p/T \in [1.6, 5.0]$ and an overpopulation elsewhere.

To quantify the difference between $f_{\text{ZPC}}(p, \tau)$ and $f_{\text{Theory}}(p, \tau)$, we calculate the relative mean deviation (RMD) between the two distributions as

$$\text{RMD}(\tau) = \sqrt{\frac{\sum_i [N_{\text{ZPC}}(p_i, \tau) - N_{\text{Theory}}(p_i, \tau)]^2}{\sum_i [N_{\text{Theory}}(p_i, \tau)]^2}}, \quad (7)$$

where $N(p_i, \tau) \propto f(p_i, \tau) \int_a^b d^3p \propto f(p_i, \tau) p_i^2$ is the number of partons in the i_{th} momentum bin from all events for the given configuration. For two distributions that differ at each momentum bin by the same fraction (ϵ or $-\epsilon$), we would have $\text{RMD} = \epsilon$. On the other hand, if a momentum distribution (with $\Delta p = T/4$) is different from the equilibrium distribution f_{eq} (or the initial distribution) only due to statistical fluctuations, we expect $\text{RMD} \simeq 4.6/\sqrt{N}$ (or $4.4/\sqrt{N}$), where N is the total number of partons in all simulated events of a configuration (16 million here). Note that these RMD values due to statistical fluctuations are $\propto 1/\sqrt{\Delta p/T}$, while the RMD value due to “real” differences in momentum distributions is essentially independent of the bin width of p/T .

In Fig. 2(a), we compare the RMD versus τ for ZPC calculations under the t -minimum scheme at several χ values (at $T = 0.5$ GeV). At early times ($\tau < 1$), the ZPC results agree very well with the exact solution results for all the shown opacities, and the deviations are consistent with the two differing by only statistical fluctuations. Figure 2(a) also shows that the RMD value generally increases with time for $\tau > 1$ until it reaches an equilibrium value around $\tau = 40$. Notably, the increase and equilibrium value of RMD do not depend monotonically on χ , consistent with the behavior of $\text{var}(p_T)$ seen earlier [30].

To further improve the ZPC accuracy, we generalize the collision scheme by introducing a parameter r in the collision time (also chosen as the ordering time):

$$t_c = \min(t_{c,1}, t_{c,2}) + r |t_{c,1} - t_{c,2}|. \quad (8)$$

So the original ZPC t -average collision scheme corresponds to $r = 1/2$ [17], while the new t -minimum collision scheme corresponds to $r = 0$ [30]. It is natural to expect the collision time to be in-between $t_{c,1}$ and $t_{c,2}$, i.e., $0 \leq r \leq 1$. We then run ZPC at a given χ value to find the r value that minimizes the relative mean deviation. Since the RMD depends on the evolution time, we choose to minimize either the equilibrium RMD value at $\tau = 60$ (RMD_{eq}) or the maximum RMD value over all τ from 0 to 60 (RMD_{max}); we call the collision scheme

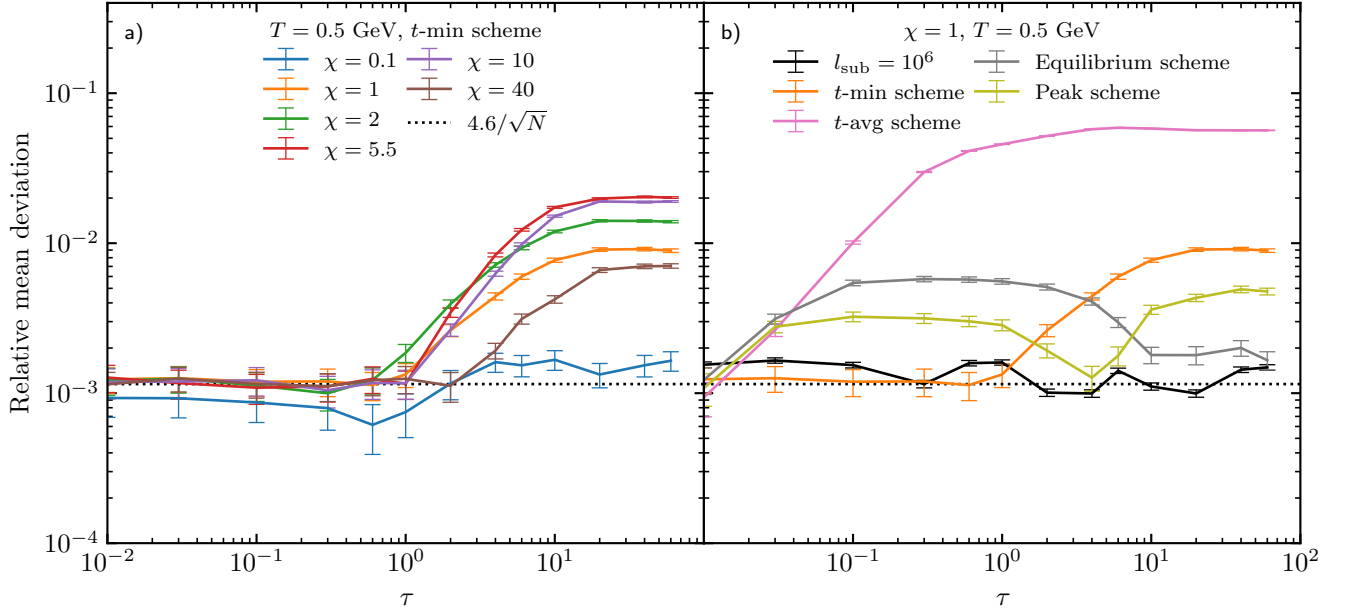


FIG. 2. Time evolution of the relative mean deviation from ZPC for a gluon gas at $T = 0.5$ GeV from (a) the t -minimum scheme at various χ values and (b) several collision schemes at $\chi = 1$. The subdivision result with $l_{\text{sub}} = 10^6$ (black) and the expectation from pure statistical fluctuations (dotted) are also shown, and the values at $\tau = 0$ have been plotted at $\tau = 10^{-2}$.

corresponding to the former as the equilibrium scheme and that corresponding to the later as the peak scheme.

We plot in Fig. 3 the r -dependence of RMD at equilibrium for various opacities. We see that for each opacity there is a r value (r_{optimal}) between 0 and 1/2 that minimizes the RMD, while the r_{optimal} value decreases as χ increases. In addition, the equilibrium RMD value at $r = 1/2$ is higher than that at $r = 0$ for each opacity, consistent with the earlier finding that the t -minimum scheme is more accurate than the original t -average scheme [30]. Note that the non-monotonic χ -dependence of the equilibrium RMD for the t -minimum scheme is already shown in Fig. 2(a), and the non-zero r_{optimal} values shown in Fig. 3 mean that indeed the accuracy of ZPC can be further improved. The RMD_{max} results versus r for the peak collision scheme are similar to Fig. 3, except that the r_{optimal} values are smaller. Also note that the RMD values at each opacity shown here (and in Fig. 5) correspond to the average of the RMD values for two temperatures $T = 0.2$ and 0.5 GeV, although the results for the two temperatures are essentially the same. After obtaining the r_{optimal} values at multiple opacities, we fit them and obtain the following parametrization of r_{optimal} as a function of χ for both the equilibrium scheme and peak scheme:

$$r_{\text{optimal}}(\chi) = \begin{cases} \frac{873}{(15.8+\chi)^{3.40}}, & \text{equilibrium scheme;} \\ \frac{518}{(15.8+\chi)^{3.40}}, & \text{peak scheme.} \end{cases} \quad (9)$$

In Fig. 2(b), we show the τ -evolution of the RMD for

four collision schemes for a gluon gas at $T = 0.5$ GeV and $\chi = 1$. We also show the ZPC results using the new parton subdivision method [30] with the subdivision factor $l_{\text{sub}} = 10^6$ as well as the expectation for pure statistical fluctuations. We see that both generalized collision schemes yield a significantly lower RMD value at equilibrium than the t -minimum scheme, while all of them give RMD values much lower than the original t -average scheme at finite times (when $\tau > 0.1$). We note that unfortunately the two generalized collision schemes both give higher relative mean deviations than the t -minimum scheme at intermediate times when $\tau \in (0.03, 1.6)$.

Figure 4 shows the ratio $f_{\text{ZPC}}(p, \tau)/f_{\text{Theory}}(p, \tau)$ at equilibrium ($\tau = 60$) for gluons in a box at $T = 0.5$ GeV and three opacities, where the ZPC results from both the t -minimum scheme and the equilibrium scheme of Eq. (9) are shown. Note that the theoretical $f_{\text{Theory}}(p, \tau)$ values have been bin-averaged as done for Fig. 1. We see that the ZPC momentum distributions in equilibrium from both schemes are very close to the theoretical distribution at low opacity ($\chi = 0.1$); this is expected since the causality violation in the parton cascade at this opacity is very small. At high opacities, however, the ZPC distribution from the t -minimum scheme can deviate significantly from the theoretical distribution. We also see that the equilibrium scheme strongly suppresses the deviations for most of the momentum range ($p/T > 1$), although it tends to underestimate the equilibrium distribution at $p/T \lesssim 1$.

To summarize the accuracy of various collision

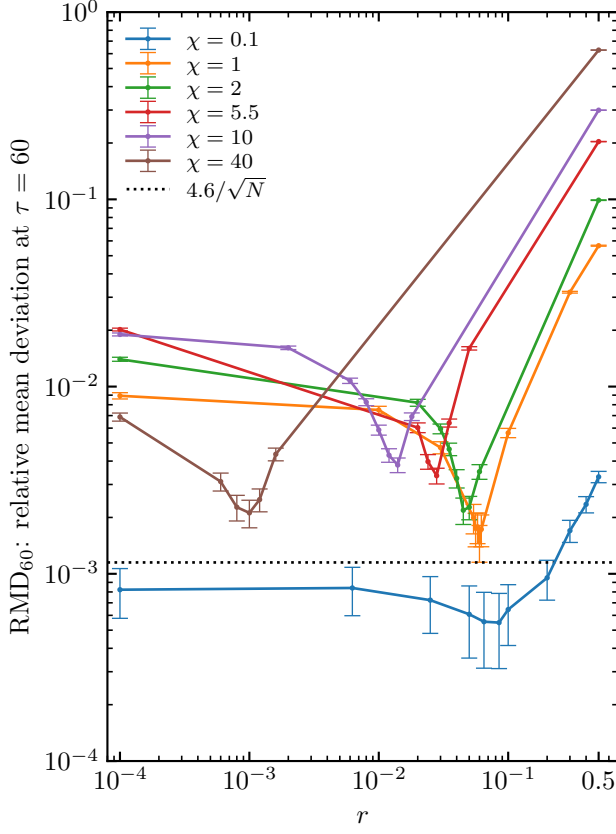


FIG. 3. The relative mean deviation at equilibrium ($\tau = 60$) versus the r parameter for various opacities. Note that the values at $r = 0$ are plotted at $r = 10^{-4}$.

schemes, we plot in Fig. 5 their RMD values versus opacity. While the original t -average scheme shows a monotonic increase of the RMD value at equilibrium from $\chi = 0.1$ to $\chi = 40$, the other three schemes all show a RMD peak (around χ between 5 and 10) with much lower magnitudes. It is also clear that the two generalized schemes of Eq. (9) are more accurate than the t -minimum scheme. For moderate to high opacities ($\chi \geq 1$), the equilibrium scheme reduces the equilibrium RMD value by a factor of 3 to 6. The red curve shows the maximum RMD value (throughout the time evolution) from the peak scheme for each opacity. Since the maximum RMD value for the t -minimum scheme always happens at or close to equilibrium (as shown in Fig. 2), Fig. 5 shows that the peak scheme reduces the maximum RMD value by a factor of ~ 2 at moderate to high opacities ($\chi \geq 1$) when compared to the t -minimum scheme.

Figure 5 also shows the relative difference between the variance of the ZPC p_T distribution in equilibrium from the t -minimum scheme and the expectation from the thermal distribution. Here, the variance is $\text{var}(p_T) = \langle p_T^2 \rangle - \langle p_T \rangle^2$, and its theoretical expectation is $(8 - 9\pi^2/16)T^2$ for massless partons under the Boltz-

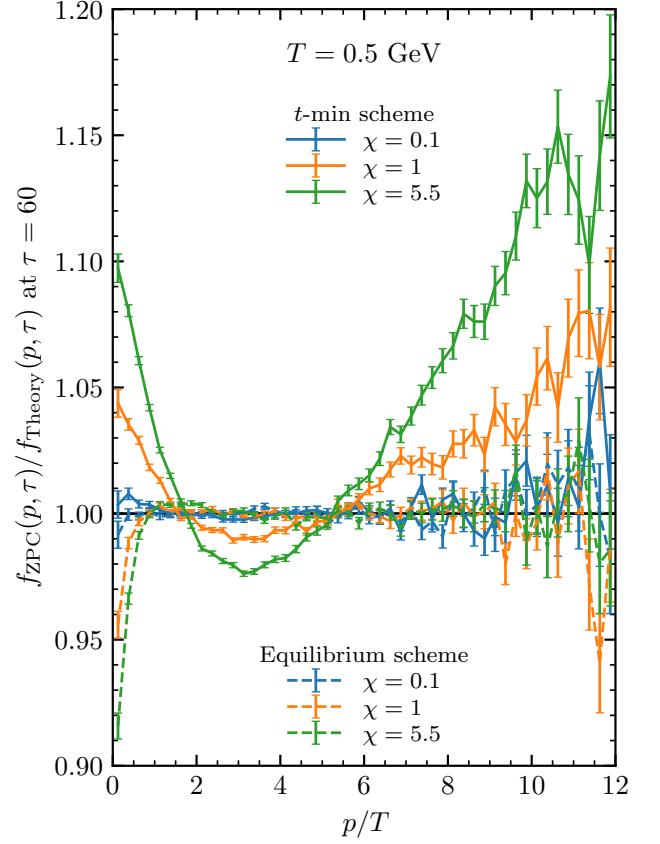


FIG. 4. Ratio of the ZPC momentum distribution at equilibrium ($\tau = 60$) over the theoretical distribution versus p/T at several opacities from the t -minimum scheme and equilibrium scheme for a gluon gas at $T = 0.5$ GeV.

mann distribution. For comparison, the $\text{var}(p_T)$ results from an earlier ZPC study [30] are also shown here, which agree with our current results after considering the estimated error bars of the earlier results. We see that the relative difference of $\text{var}(p_T)$ versus opacity from the t -minimum scheme closely follows the shape of the relative mean deviation but are higher in magnitude. Like the relative mean deviations for three out of four collision schemes, the relative difference of $\text{var}(p_T)$ also peaks at χ between 5 and 10.

CONCLUSION

Transport models based on the kinetic theory are important tools for the study of non-equilibrium dynamics in nuclear collisions including the origin of collectivity from small to large colliding systems. It is thus essential for a parton transport to be able to solve the relativistic Boltzmann equation accurately. Preferably this should be achieved without using the parton subdivision method, which alters the event-by-event correlations and

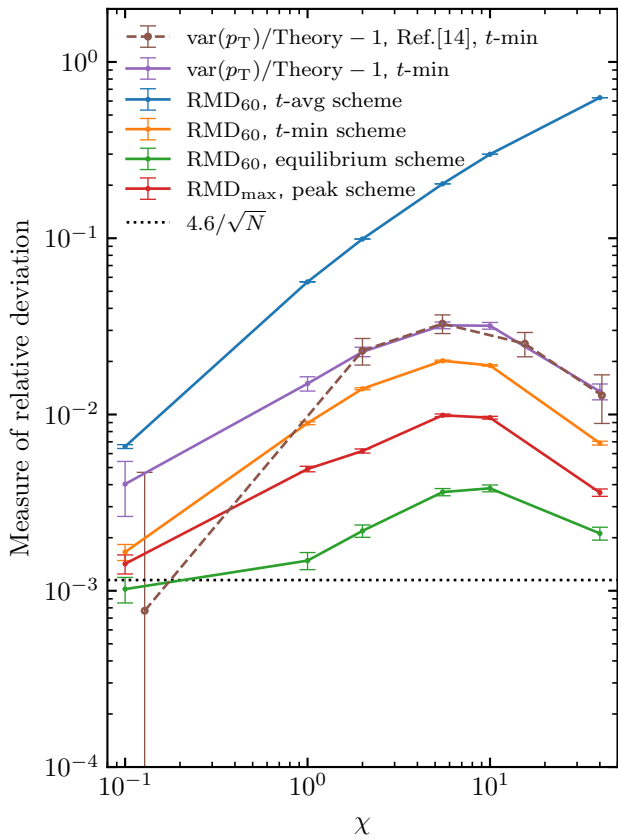


FIG. 5. The relative mean deviation in equilibrium (RMD_{60}) for three collision schemes of ZPC, in addition to the relative deviation of the variance of the momentum distribution in equilibrium from the t -minimum scheme, as functions of the opacity. The maximum relative mean deviation for all τ (RMD_{max}) from the peak scheme (red) and the expectation from pure statistical fluctuations (dotted) are also shown.

fluctuations. In this study, we first examine and then improve the ZPC parton cascade for gluons under isotropic elastic scatterings in a box with periodic boundary conditions. By comparing the results with an exact analytical solution of the relativistic Boltzmann equation for a given initial condition, we can for the first time quantify the parton cascade accuracy in the full momentum distribution throughout the time evolution. We first confirm that, compared to the original t -average collision scheme, the recent t -minimum collision scheme significantly improves the accuracy, leading to a relative mean deviation of $\lesssim 2\%$ in equilibrium for all opacities. We then generalize the collision scheme to be opacity-dependent to further improve the accuracy, where the peak scheme has a relative mean deviation of $\leq 1\%$ for the momentum distribution at any time for all opacities (up to $\chi = 40$). These levels of accuracy at high opacities ($\chi > 1$) are noteworthy because naively the parton cascade is expected to fail there. An accurate parton cascade for box calcula-

tions lays the foundation to apply and assess the parton cascade in more realistic 3-dimensional expansion cases.

ACKNOWLEDGEMENT

This work has been supported by the National Science Foundation under Grant No. 2012947 and 2310021. We thank Dr. M. Martinez for discussions about the exact solution. We would like to acknowledge the use of the following software: Matplotlib [35], Numpy [36], Scipy [37].

* linz@ecu.edu

- [1] J. Adams et al. (STAR), Nucl. Phys. A **757**, 102 (2005).
- [2] B. Abelev et al. (ALICE), J. Phys. G **41**, 087002 (2014).
- [3] M. S. Abdallah et al. (STAR), Phys. Lett. B **827**, 137003 (2022).
- [4] STAR (2025), 2504.02531.
- [5] D. Molnar and S. A. Voloshin, Phys. Rev. Lett. **91**, 092301 (2003).
- [6] A. Adare et al. (PHENIX), Phys. Rev. Lett. **114**, 192301 (2015).
- [7] C. Aidala et al. (PHENIX), Nature Phys. **15**, 214 (2019).
- [8] M. I. Abdulhamid et al. (STAR), Phys. Rev. Lett. **130**, 242301 (2023).
- [9] V. Khachatryan et al. (CMS), JHEP **09**, 091 (2010).
- [10] V. Khachatryan et al. (CMS), Phys. Rev. Lett. **115**, 012301 (2015).
- [11] M. P. Heller and M. Spalinski, Phys. Rev. Lett. **115**, 072501 (2015).
- [12] A. Kurkela, U. A. Wiedemann, and B. Wu, Phys. Lett. B **783**, 274 (2018).
- [13] A. Kurkela, W. van der Schee, U. A. Wiedemann, and B. Wu, Phys. Rev. Lett. **124**, 102301 (2020).
- [14] L. He, T. Edmonds, Z.-W. Lin, F. Liu, D. Molnar, and F. Wang, Phys. Lett. B **753**, 506 (2016).
- [15] Z.-W. Lin, L. He, T. Edmonds, F. Liu, D. Molnar, and F. Wang, Nucl. Phys. A **956**, 316 (2016).
- [16] K. Li, H.-F. Song, H.-J. Xu, Y.-L. Sun, and F. Wang (2024), 2405.02847.
- [17] B. Zhang, Comput. Phys. Commun. **109**, 193 (1998).
- [18] Z. Xu and C. Greiner, Phys. Rev. C **71**, 064901 (2005).
- [19] A. Kurkela, R. Törnkvist, and K. Zapp, Eur. Phys. J. C **84**, 74 (2024).
- [20] A. Kurkela, A. Mazeliauskas, J.-F. Paquet, S. Schlichting, and D. Teaney, Phys. Rev. C **99**, 034910 (2019).
- [21] H. Sorge, H. Stoecker, and W. Greiner, Annals Phys. **192**, 266 (1989).
- [22] S. A. Bass et al., Prog. Part. Nucl. Phys. **41**, 255 (1998).
- [23] H.-T. Janka, K. Langanke, A. Marek, G. Martinez-Pinedo, and B. Mueller, Phys. Rept. **442**, 38 (2007).
- [24] W. Florkowski, R. Ryblewski, and M. Strickland, Nucl. Phys. A **916**, 249 (2013).
- [25] T. Kodama, S. B. Duarte, K. C. Chung, R. Donangelo, and R. A. M. S. Nazareth, Phys. Rev. C **29**, 2146 (1984).
- [26] G. Kortmeyer, W. Bauer, K. Haglin, J. Murray, and S. Pratt, Phys. Rev. C **52**, 2714 (1995).
- [27] R. Törnkvist and K. Zapp, Phys. Lett. B **856**, 138952 (2024).

- [28] B. Zhang, M. Gyulassy, and Y. Pang, Phys. Rev. C **58**, 1175 (1998).
- [29] D. Molnar and M. Gyulassy, Phys. Rev. C **62**, 054907 (2000).
- [30] X.-L. Zhao, G.-L. Ma, Y.-G. Ma, and Z.-W. Lin, Phys. Rev. C **102**, 024904 (2020).
- [31] M. Krook and T. T. Wu, Phys. Rev. Lett. **36**, 1107 (1976).
- [32] D. Bazow, G. S. Denicol, U. Heinz, M. Martinez, and J. Noronha, Phys. Rev. Lett. **116**, 022301 (2016).
- [33] D. Bazow, G. S. Denicol, U. Heinz, M. Martinez, and J. Noronha, Phys. Rev. D **94**, 125006 (2016).
- [34] J. Tindall, J. M. Torres-Rincon, J. B. Rose, and H. Petersen, Phys. Lett. B **770**, 532 (2017).
- [35] J. D. Hunter, Computing in Science & Engineering **9**, 90 (2007).
- [36] C. R. Harris et al., Nature **585**, 357 (2020).
- [37] P. Virtanen et al., Nature Meth. **17**, 261 (2020).